Induction of non-lamellar phases in archaeal lipids at high temperature and high hydrostatic pressure by apolar polyisoprenoids

Marta Salvador-Castell, Nicholas Brooks, Judith Peters, P. Oger

Induction of non-lamellar phases in archaeal lipids at high temperature and high hydrostatic pressure by apolar polyisoprenoids

Marta Salvador Castell[a], Nick Brooks[b], Judith Peters[c,d] & Philippe Oger[a]

a. Université de Lyon, INSA de Lyon, CNRS, UMR 5240, 69211 Villeurbanne, France.

b. Imperial College London, South Kensington Campus, London SW7 2AZ, England

c. Université Grenoble Alpes, LiPhy, CNRS, 38000 Grenoble, France

d. Institut Laue Langevin, 38000 Grenoble, France

Abstract

It is now well established that cell membranes are much more than a barrier that separate the cytoplasm from the outside world. Regarding membrane's lipids and their self-assembling, the system is highly complex, for example, the cell membrane needs to adopt different curvatures to be functional. This is possible thanks to the presence of non-lamellar-forming lipids, which tend to curve the membrane. Here, we present the effect of squalane, an apolar isoprenoid molecule, on an archaea-like lipid membrane. The presence of this molecule provokes negative membrane curvature and forces lipids to self-assemble under inverted cubic and inverted hexagonal phases. Such non-lamellar phases are highly stable under a broad range of external extreme conditions, e.g. temperatures and high hydrostatic pressures, confirming that such apolar lipids could be included in the architecture of membranes arising from cells living under extreme environments.

Introduction

Since Singer and Nicolson[1] first defined the membrane as a mosaic of proteins and lipids in a lamellar fluid liquid-crystalline (L_α) phase, our view of the membrane ultrastructure has become more sophisticated, recognizing the existence of membrane domains of specific lipid composition in natural membranes. Each composition corresponds to a particular phase, which play important roles in cell membrane function and cell physiology as they have very specific physicochemical properties, such as different lateral motions, rotations, fluidity, and phase structuration, and promote the formation of lamellar or non-lamellar phase[2,3].

Lamellar, cubic and inverted hexagonal phases possess different bending fluctuations and intrinsic curvatures4, which are mostly defined by the shape of the lipids present in the membrane. This has been rationalized using the critical geometric packing parameter (P) concept, which defines P as $v(a*l)^{-1}$ where v is the molecular volume, l is the molecular length and a is the molecular area at the lipid-water interface[5,6]. For P<1, molecules are inverted cones and tend to produce positive curvatures, i.e. the hydrocarbon chains are closest to each other. For P ≈ 0, lipids have a cylindrical shape and adopt zero curvature, giving rise to lamellar phases. For P>1, lipids present conical shapes and adopt negative curvatures and self-assemble under the so-called inverted phases, such as the cubic (Q) and hexagonal (H_{II}) phases, simply to release their curvature frustration (Figure 1). Changes between lamellar and non-lamellar former lipid compositions tune the flexibility and curvature of the membrane[7] which is used by cell to tune its membrane functionality by adjusting its membrane lipid compositions to adapt itself and maintain essential functions under different environmental conditions.

Archaeal phospholipids present unique characteristics: a *sn*-glycerol-1-phosphate (G-1-P) backbone, ether linkages, and isoprenoid hydrocarbon chains[8]. The methyl groups along the acyl chains are responsible for the fact that both phospholipid's rotamers are nearly energetically equivalent9, thus allowing archaeal lipids to occur in the Lα phase for a broad range of

temperature (-120°C to 120°C)[9,10]. Isoprenoid chains pack densely, increase membrane viscosity and decrease its water permeability[11–13]. The presence of ether bounds, isoprenoid hydrocarbon chains and transmembrane lipids is thought to be the reason of the incredibly high resistance of archaeal cell membranes to extreme conditions[14]. For example, some Archaea have their optimal growth conditions at low pH, high salinity, high temperature (HT) and/or high hydrostatic pressure (HHP), including a highly stable and selective permeable cell membrane. Intriguingly, liposomes made from archaeal lipids present highly irregular shapes[15] and indeed, extracellular membrane vesicles are highly produced by Archaea[16]. All these findings indicate that non-lamellar-forming lipids may play a particular important role in the Archaea domain.

The geometric packing parameter predicts that most archaeal phospholipids will have zero or positive curvatures which will not favour the formation of the non-lamellar phases indispensable for biological activity. This is for example the case for the membrane lipids of *Thermococcus barophilus* which have phosphatidyl inositol polar headgroup and derivatives of this polar headgroup. Recently, Cario and colleagues[17] proposed a novel archaeal membrane architecture for the hyperthermophile and piezophile Archaeon *T. barophilus* in order to explain its ability to thrive at temperatures close to 100°C[18]. According to this hypothesis, apolar isoprenoid molecules would populate the hydrophobic space between the two bilayer leaflets, thus modifying the membrane properties, decreasing permeability to proton and water and membrane rigidity[19]. In addition, the presence of the interleaving molecules within the plane of the membrane is proposed to be implied in modifying the phases transition in the membrane. Indeed, the partitioning of non-polar molecules, such as alkanes, aromatic compounds and isoprenoid chains into the hydrocarbon region, increases the tendency of the lipid layer to adopt a negative interfacial curvature[20–22]. Therefore, lipids reduce their hydrocarbon packing stress self-assembling within inverted non-lamellar phases. For example, the addition of 5% alkane to a mixture of PC/PE-lipids reduces the L_{α}-H_{II} transition by 55°C[23]. To date, the effect of apolar lipids on archaeal membranes has not been studied.

Using Small Angle X-ray Scattering (SAXS), we have determined the lipid phases from a mixture of archaeal lipids in presence of different molar percentages (mol%) of the polyisoprenoid squalane at different temperatures and pressures. Here we show that in absence of the apolar intercalant, the archaeal lipids cannot form non-lamellar phases, and that the presence of the apolar molecule imposes highly stable non-lamellar type II Q and H phases.

Experimental section

I. Chemicals

The high purity (>99%) synthetic archaeal lipids 1,2-di-O-phytanyl-*sn*-glycero-3-phosphocholine (DoPhPC) and 1,2-di-O-phytanyl-*sn*-glycero-3-phosphoethanolamine (DoPhPE) were purchased from Avanti Polar Lipids in the lyophilized form and utilized without further purification. 2,6,10,15,19,23-Hexamethyltetracosane (squalane) was bought from Alfa Aesar.

II. Small angle X-ray diffraction

SAXS experiments were performed on beamline I22[24] at the Diamond Light Source (United Kingdom). DoPhPC and DoPhPE were used in a proportion 9:1 molar. Phospholipids with contents of 20% (w/v water) and the adequate quantity of squalane (1%, 2.5%, 5% and 10% molar) were placed inside a pressure chamber[25]. The pressure and temperature dependent experiment was carried out at six different temperatures (10°C, 25°C, 40°C, 55°C, 70°C and 85°C) in pressure jumps of 50 bar from 0 bar to 1000 bar.

The X-ray energy was 18 keV, the momentum transfer is defined as $q = 4\pi * \sin(\Theta)/\lambda$, where 2θ is the scattering angle. The small-angle regime was $0.005 < q < 0.35$ Å-1. The type of phase can be distinguished by the characteristic SAXS peak ratios26: for a lamellar phase they are equidistant, for a hexagonal phase they are: 1, $\sqrt{3}$, 2, $\sqrt{7}$…, for a cubic phase Pn3m they are: $\sqrt{2}$, $\sqrt{3}$, 2, $\sqrt{6}$, $\sqrt{8}$, 3… and for a cubic phase Im3m they are: $\sqrt{2}$,2,$\sqrt{6}$, $\sqrt{8}$, 3... The lattice parameter

a is defined as a_{lam}= 2π/q_n and a_{hex}= (2π/q_n)*2/3 for a lamellar and a hexagonal phase, respectively. To determine the lattice parameter for the cubic phase, the experimentally obtained peak position s, where s= 2*sin (Θ)/λ = q/2π, is plotted vs $(h^2 + k^2 + l^2)^{1/2}$, where h,k,l are the Miller indices by which the peaks are indexed. The plot should intercept through the origin and be linear with a slope of 1/acubic.

Results and discussion

I. Archaeal phospholipids self-organize under lamellar phases

Lipid phases in excess of water can be identified by the relative Bragg peak positions in the SAXS patterns[26]. Collected data points and phase diagrams are shown in Figure 2. In absence of the apolar molecule, only lamellar phases can be identified in the SAXS spectra (Salvador Castell, unpublished results). At 10°C and ambient pressure, the lattice parameter of the lamellar phase is 62.7 ± 0.6 Å. As expected, the lamellar phase appears sensitive to HT (Figure S1). The lattice parameter increases at least to the highest temperature tested of 85°C. However, starting from 70°C the sample loses its correlation between bilayers and becomes so disordered that only the first diffraction order can be fitted with accuracy. The lattice parameter increases from 62.7 ± 0.6 Å at 10°C to 73.2 ± 1 Å. The lamellar phase appears little sensitive to hydrostatic pressure. Indeed, the lattice parameter varies only within the error bars of the measure. In contrast to other lipid systems in which hydrostatic pressure exert a structuring impact on the bilayers[27], we see no such effect on DoPhPC:DoPhPE-based membranes. In fact, at the highest combined pressures and temperatures (85°C and >750 bar), no diffraction peaks are visible anymore.

II. Addition of 1 mol% squalane induces the formation of inverted non-lamellar phases

Upon addition of squalane, even at the smallest quantity of 1 mol%, we observed the presence of non-lamellar phases of type II, in co-existence or not with lamellar phases, which suggests that the presence of squalane increases the negative membrane curvature (Salvador Castell, unpublished results). At all temperatures, we observe a cubic phase, in coexistence with a lamellar phase up to 40°C and a hexagonal phase above. In contrast to the lipid system without squalane, the system with 1mol% squalane is both pressure and temperature sensitive. The a_{lam} increases as a function of HHP from 67.6 ± 0.3 Å at ambient pressure to 69.8 ± 0.3 Å at 1000 bar at 10°C for example, but also as a function of temperature where it reaches 69.6 ± 0.5 Å at 40°C and 1 bar (Figure S2). Temperature is known to favour the negative intrinsic curvature of the lipid self-assembly. At temperatures of 55°C and above, a mixture of a Pn3m cubic phase and an inverted hexagonal phase coexist. At 85°C, three different Pn3m phases with very slightly different lattice values coexist, which is indicative that they have most likely different hydration levels (Figure 3). Note the substantial lattice parameters of the cubic phases (a_{Pn3m} = 254 ± 2 Å and a_{Im3m} = 332 ± 3 Å) which reflect the high potential of squalane to reduce chain packing frustration. Values for the lattice parameter for bacterial lipid cubic phases are substantially smaller, such as 105 Å for monoolein (MO) [28,29] or 122 Å for 1,2-dioleoyl-sn-glycero-3-phosphoethanolamine (DOPE)[30]. However, under certain conditions this lattice parameter can reach values higher than those measured here, an example is the case of a diphytanoyl PC-cholesterol mixture, in which the Q_{II} phase has a a_{cubic} of 510 Å[31]. At 85°C, we observe the replacement of the Pn3m by the Im3m phase (Figure 3). Thus remarkably, HHP leads to the replacement of a Pn3m cubic phase with a lower a_{cubic} and higher negative curvature to a Im3m's cubic phase with a higher a_{cubic} and lower negative membrane curvature. In accordance with geometric considerations for those coexisting phases[32,33], we found that the ratio between their lattice parameters is 1.28. The hexagonal phase has a lattice parameter ranging from 87.9 ± 0.5

147 Å at 55°C to 80.1 ± 0.5 Å at 85°C under ambient pressure. This a_{hex} is highly sensitive to pressure,
148 ranging from 82.2 ± 0.5 Å at 1 bar to 90.1 ± 0.5 Å at 1000 bar at 70°C for example. This is in
149 accordance with the fact that non-lamellar self-assemblies easily swell at HHP[34]. In addition, such
150 a_{hex} is much higher than the a_{hex} usually obtained for familiar lipids which lie at 52.9 Å at 97°C
151 for MO[35] or 65.8 Å at 70°C for DOPE[36], for example. This may be directly related to the ability of
152 squalane to release the chain frustration at H_{II} phases with high a_{hex}.

153 **III. Higher negative curvature in presence of 2.5 mol% of squalane**

154 By further adding squalane, the system presents a coexistence of a lamellar and HII phases at
155 low temperature and no longer a coexistence of lamellar and cubic phases, which is indicative
156 of a further increase of the membrane negative curvature. As for the 1 mol% squalane lipid
157 system, the lamellar phase is present up to 40°C, but in contrast, it seems to be far less sensitive
158 to pressure (Figure S3). At 85°C, the hexagonal phase coexists with two cubic phases, probably
159 Im3m. Remarkably, at 55°C and 70 °C, HHP induces a phase transition to a second hexagonal
160 phase coexisting with the one already presented at low pressures (Figure 4a). We propose that
161 this phase separation could result from the rearrangement of squalane between a squalane rich
162 and a squalane poor phase. As observed before, the hexagonal phase is much more sensitive to
163 temperature and HHP than the lamellar phase. The a_{hex} decreases from 94.6 ± 0.5 Å at 10°C to
164 77.4 ± 0.5 Å at 85°C at 1 bar and increases from 94.6 ± 0.5 Å to 103.1 ± 0.5 Å at 1 bar to 1000
165 bar at 10°C (Figure S3b). Last, at 85°C, two pressure-sensitive Im3m phases appear in
166 coexistence with the H_{II} phase (Figure 4b). The a_{cubic} varies from 248 ± 2 Å and 264 ± 2 Å at 1 bar,
167 to 264 ± 2 Å and 279 ± 2 Å, at 1000 bar for the two phases (Figure S3c). The presence of these
168 two Q_{II} phases may be due to different hydration levels as observed at 1 mol% squalane.

169

170

IV. A competition between lamellar and inverted hexagonal phase appears by adding 5 mol% squalane

In presence of 5 mol% squalane at 1 bar, the system presents a mixture of one lamellar and one inverted hexagonal phase at temperatures up to 55°C (Figure 5a). As expected, temperature increases the membrane's negative curvature and at 70°C and above only the HII is present. In contrast, pressure promotes the lamellar phase, which can be readily observed at 70°C, where the lamellar phase appears above 350 bar. Higher HHP values further increase the structuration of the lamellar phase (Figure 5b). At their highest temperature tested, e.i. 85°C, the lamellar phase appears at 1000 bar. In presence of 5 mol% squalane, the lamellar-to-hexagonal transition is a direct conversion as no cubic phase appears.

Interestingly, HHP swells much more the HII phase than the lamellar one. At 10°C, a_{lam} remains almost constant at 57.8 ± 0.4 Å – 58.0 ± 0.4 Å from 1 bar to 1000 bar but, due to the capability of squalane to reduce chain frustration, the hexagonal phase is able to swell from 111.8 ± 0.5 Å at 1 bar to 121.2 ± 0.5 Å at 1000 bar for the same temperature (Figure 5c and Figure S4).

The different pressure sensitivities of the L and HII phases are easily observed when plotting Δa, e.i. the difference between the lattice parameter at HHP and at ambient pressure (Figure 6a). The Δa of the lamellar phase is ca. 0.2 Å*kbar^{-1} and not significative. In contrast, the HII phases swell up to 9.5 Å*kbar^{-1} at 10°C and 1.5 Å*kbar^{-1} at 85°C. Familiar Lα phases usually swell up to 2 Å*kbar^{-1} while H_{II} may swell as much as 6 Å*kbar^{-1} [34]. The swelling of HII decreases with temperature. This unexpected behaviour can be explained by the coexistence of the HII and lamellar phases in the system. Indeed, one can observe the change of slope of Δa at 70°C and 450 bar (Figure 6b), which coincides with the appearance of the lamellar phase in this lipid system: in absence of the lamellar phase, Δa is ~ 1 Å*kbar^{-1}, in presence of the lamellar phase it increases to 5.2 Å*kbar^{-1}. At 85°C, at which no lamellar phase is observed below 1000 bar, the slope of Δa remains close to 1 Å*kbar^{-1}. Such differences may be explained by the partition of

two polar headgroups and the apolar molecule squalane between the two phases in coexistence. Indeed, in this lipid mixture we have two lipids with very different curvature. Phospholipids containing PC headgroups present a zero-curvature monolayer and self-assemble in a lamellar phase. DoPhPE easily bends under negative curvatures and therefore induce the formation of inverted non-lamellar phases, such as the H_{II}. Accordingly, when L and HII phases are present, the system may present a "lipid-separation" and DoPhPE may have the tendency to adopt the HII phase with its preferred curvature. When the lamellar phase is present, as at 70°C and pressures above 450 bar, DoPhPE may principally form the HII phase (Figure 6c). This effect was already observed in bacterial-like lipids, which better accommodate in L_β or L_α phases. For example, a decrease in temperature induces domains enriched in saturated phospholipids with small quantities of unsaturated lipids[37]. As DoPhPE has a higher lateral compressibility, HII presents a higher Δa slope when most of DoPhPE is partitioned in the non-lamellar phase and excluded from the L phase. However, the presence of methyls in the hydrocarbon chains could reduce the lateral diffusion of these phospholipids and squalane may aggregate in the chain frustration points and most especially at the interphase points, to fill the voids and release packing tension. The chain-packing frustration increases as the diameter of the hexagonally packed cylindrical inverse micelles increases. When the lamellar phase disappears, the apolar molecule can better distribute along the HII phase and squalane aggregates may disappear (Figure 6c). Therefore, the lattice parameter of the HII phase decreases and consequently its pressure response.

V. Only the inverted hexagonal phase is present when 10 mol% squalane is added

At 10 mol% squalane in the DoPhPC:DoPhPE (9:1) mixture only the HII phase is observed under all temperatures and pressures studied. At ambient pressure, we could detect a slow phase

transition between two HII phases. The axially integrated 1-D patterns at 55°C, 70°C and 85°C (Figure 7a) shows the apparition of a HII phase at higher q and the gradual disappearance of the peaks characteristics of the second hexagonal phase. The spectrum at 85°C stills shows shoulders corresponding to the low temperature HII phase. The lattice parameters of HII range from 104.8 ± 0.5 Å at 10°C and 1 bar to 92.8 ± 0.5 Å at 85°C and 1 bar (Figure 7c and Figure S5). As thermal motions increase lipid dynamics, the HII phase is much more pressure sensitive at HT (Figure 7b and 7c). Δa expansion increases from 0.1 Å*kbar^{-1} at 10°C to 3.9 Å*kbar^{-1} at 85°C (Figure 7d). One can notice that the Δa curve as a function of pressure at 40°C presents 2 slopes, consistent with a phase transition between two hexagonal phases. This phase transition also possibly occurs at lower temperature, although very close to 1 bar. Such phase transition is not visible at temperatures above 40°C. These low hexagonal phases differ principally by their ability to swell with pressure, which is congruent with a higher pressure-dependent lateral compressibility of the high temperature hexagonal phase.

Conclusions

X-ray diffraction experiments clearly show that the addition of squalane drastically changes membrane curvature of a lipid DoPhPC:DoPhPE (9:1) mixture, an effect comparable to that of cholesterol at biological relevant quantities on eukaryote-like lipids[38,39]. SAXS data displays the presence of highly stable non-lamellar lipid phases dependent on mol% of squalane, temperature and pressure. The complete understanding of the observed structural transitions will require a deeper study as it will be necessary to consider different kind of interactions, such as lipid-water, lipid-lipid and lipid-squalane. However, the outstanding acubic values and resistance revealed by the system may be useful for the stabilization or modification of cubosomes and to adjust lipid membrane properties of archaeosomes[40,41].

The fact that small quantities of squalane (1 – 10 mol%) are capable to impose negative intrinsic curvatures on the system has biological significance. Our results indicate that archaeal membranes simply require to regulate squalane proportions in the cell membrane to tune its curvature and flexibility. Therefore, due to the presence of small amounts of the apolar molecule, archaeal cells would be capable to manage essential cell processes such as fusion and fission[42]. Furthermore, recognizing that squalane is present in archaeal cell membranes and considering the high metastability of all phase transitions in a large range of temperatures and pressures, we can predict that non-lamellar phases and particularly, inverted cubic phases, may be locally present in archaeal membranes.

Conflicts of interest

There are no conflicts to declare.

Acknowledgements

This work was supported by the French National Research Agency programmes ANR 2010 BLAN 1725-04 and ANR 17-CE11-0012-01 to PO and JP and the Royal Society to PO and NB. MSC was supported by a PhD grant from the French Ministry of Research.

References

1 S. J. J. Singer and G. L. L. Nicolson, *Science (80-.).*, 1972, **175**, 720–731.

2 M. Cebecauer, M. Amaro, P. Jurkiewicz, M. J. Sarmento, R. Šachl, L. Cwiklik and M. Hof, *Chem. Rev.*, 2018, **118**, 11259–11297.

3 F. M. Goñi, *Chem. Phys. Lipids*, 2019, **218**, 34–39.

4 W. Helfrich, *Zeitschrift für Naturforsch. C*, 1973, **28**, 693–703.

5 J. N. Israelachvili, D. J. Mitchell and B. W. Ninham, *J. Chem. Soc. Faraday Trans. 2*, 1976, **72**, 1525.

6 C. V. Kulkarni, *Chem. Phys. Lipids*, 2019, **218**, 16–21.

7 B. W. Ninham, K. Larsson and P. Lo Nostro, *Colloids Surfaces B Biointerfaces*, 2017, **152**, 326–338.

8 M. De Rosa, A. Gambacorta and A. Gliozzi, *Microbiol. Rev.*, 1986, **50**, 70–80.

9 H. Lindsey, N. O. Petersen and S. I. Chan, *Biochim. Biophys. Acta*, 1979, **555**, 147–67.

10 A. Polak, M. Tarek, M. Tomšič, J. Valant, N. Poklar Ulrih, A. Jamnik, P. Kramar and D. Miklavčič, *Langmuir*, 2014, **30**, 8308–8315.

11 W. Shinoda, M. Mikami, T. Baba and M. Hato, *J. Phys. Chem. B*, 2004, **108**, 9346–9356.

12 W. Shinoda, M. Mikami, T. Baba and M. Hato, *AIP Conf. Proc.*, 2004, **708**, 352–353.

13 S. Tristram-Nagle, D. J. Kim, N. Akhunzada, N. Kuerka, J. C. Mathai, J. Katsaras, M. Zeidel and J. F. Nagle, *Chem. Phys. Lipids*, 2010, **163**, 630–637.

14 A. O. Chugunov, P. E. Volynsky, N. A. Krylov, I. A. Boldyrev and R. G. Efremov, *Sci. Rep.*, 2014, **4**, 7462.

15 D. Gmajner, P. A. Grabnar, M. T. Žnidarič, J. Štrus, M. Šentjurc and N. P. Ulrih, *Biophys. Chem.*, 2011, **158**, 150–156.

16 S. Gill, R. Catchpole and P. Forterre, *FEMS Microbiol. Rev.*, 2019, **43**, 273–303.

17 A. Cario, V. Grossi, P. Schaeffer and P. M. Oger, *Front. Microbiol.*, 2015, **6**, 1–12.

18 V. T. Marteinsson, J.-L. Birrien, A. Reysenbach, M. Vernet, D. Marie, A. Gambacorta, P. Messner, U. B. Sleytr and D. Prieur, *Int. J. Syst. Bacteriol.*, 1999, **49**, 351–359.

19 T. H. Haines, *Prog. Lipid Res.*, 2001, **40**, 299–324.

20 M. W. Tate, E. F. Eikenberry, D. C. Turner, E. Shyamsunder and S. M. Gruner, *Chem. Phys. Lipids*, 1991, **57**, 147–164.

21 K. Lohner, G. Degovics, P. Laggner, E. Gnamusch and F. Paltauf, *Biochim. Biophys. Acta*, 1993, **1152**, 69–77.

22 J. M. Seddon and R. H. Templer, 1995, **1**, 97–160.

23 G. L. Kirk and S. M. Gruner, *J. Phys.*, 1985, **46**, 761–769.

24 A. J. Smith, L. S. Davidson, J. H. Emmins, J. C. H. Bardsley, P. Holloway, M. Malfois, A. R. Marshall, C. L. Pizzey, S. E. Rogers, O. Shebanova, T. Snow, E. P. Williams and N. J. Terrill, *Preprint*.

25 N. J. Brooks, B. L. L. E. Gauthe, N. J. Terrill, S. E. Rogers, R. H. Templer, O. Ces and J. M. Seddon, *Rev. Sci. Instrum.*, 2010, **81**, 1–10.

26 A. I. I. Tyler, R. V. Law and J. M. Seddon, in *Methods in Membrane Lipids*, ed. D. M. Owen, Springer, 2015, pp. 199–255.

27 N. L. C. McCarthy and N. J. Brooks, in *Advances in Biomembranes and Lipid Self-Assembly*, Elsevier Inc., 2016, vol. 24, pp. 75–89.

28 P. Mariani, V. Luzzati and H. Delacroix, *J. Mol. Biol.*, 1988, **204**, 165–189.

29 C. V. Kulkarni, W. Wachter, G. Iglesias-Salto, S. Engelskirchen and S. Ahualli, *Phys. Chem. Chem. Phys.*, 2011, **13**, 3004–3021.

30 E. Shyamsunder, S. M. Gruner, M. W. Tate, D. C. Turner, P. T. C. So and C. P. S. Tilcock, *Biochemistry*, 1988, **27**, 2332–2336.

31 B. G. Tenchov, R. C. MacDonald and D. P. Siegel, *Biophys. J.*, 2006, **91**, 2508–2516.

32 B. Tenchov and R. Koynova, *Chem. Phys. Lipids*, 2017, **208**, 65–74.

33 B. Tenchov, R. Koynova and G. Rapp, *Biophys. J.*, 1998, **75**, 853–866.

34 N. J. Brooks, *IUCrJ*, 2014, **1**, 470–477.

35 J. Briggs, H. Chung, M. Caffrey and T. T. Phase, *J. Phys. II Fr.*, 1996, **6**, 723–751.

36 D. C. Turner and S. M. Gruner, *Biochemistry*, 1992, **31**, 1340–1355.

37 S. Baoukina, E. Mendez-Villuendas, W. F. D. Bennett and D. P. Tieleman, *Faraday Discuss.*, 2012, **161**, 63–75.

38 J. J. Cheetham, E. Wachtel, D. Bach and R. M. Epand, *Biochemistry*, 1989, **28**, 8928–8934.

39 X. Wang and P. J. Quinn, *Biochim. Biophys. Acta - Biomembr.*, 2002, **1564**, 66–72.

40 H. M. G. Barriga, M. N. Holme and M. M. Stevens, *Angew. Chemie - Int. Ed.*, 2019, **58**, 2958–2978.

41 T. Benvegnu, L. Lemiègre and S. Cammas-marion, *Recent Pat. Drug Deliv. Formul.*, 2009, **33**, 206–220.

42 H. T. McMahon and E. Boucrot, *J. Cell Sci.*, 2015, **128**, 1065–1070.

322 **Figures**

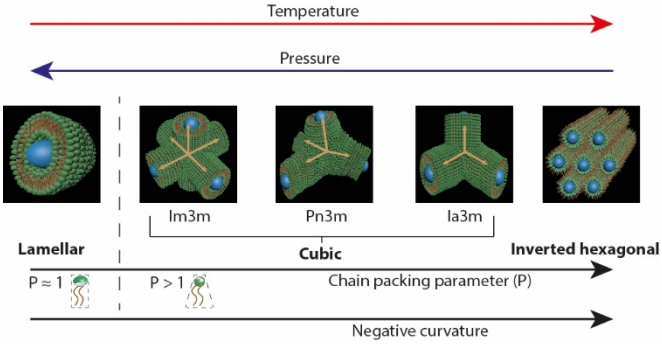

Figure 1. Schematic representation of different lipid phases as a function of lipid curvature. The lipid headgroups are represented in green, the hydrocarbon chains in brown and water location in blue. The arrows indicate the direction for the increase of the different parameters: chain packing parameter (P), negative intrinsic curvature of the membrane, pressure and temperature.

323

324

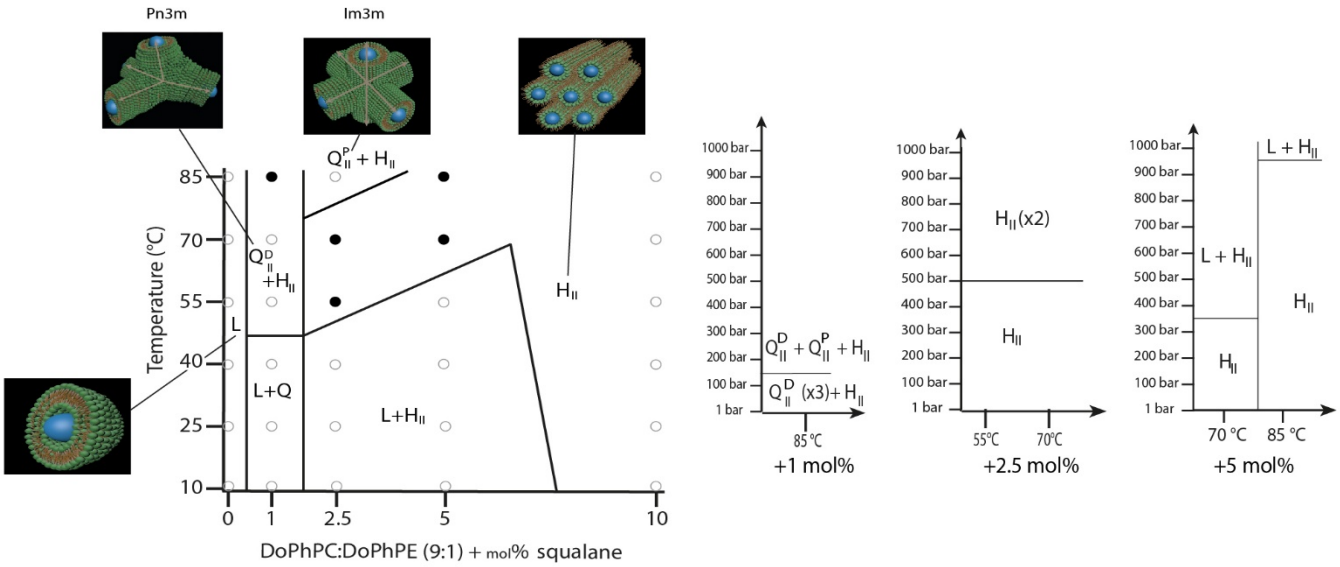

Figure 2. Phase diagrams of the DoPhPC:DoPhPE (9:1) in presence of excess water as a function of the proportion of squalane, temperature (Left panel) and pressure (Right panel) Left, sketches of each phase (same colour scheme as in figure 1). Full circles indicate conditions under which pressure-induced phase transitions are observed and detailed in the right panel, and open circles those under which no pressure-induced phase transition is observed between 0 and 1000 bar.

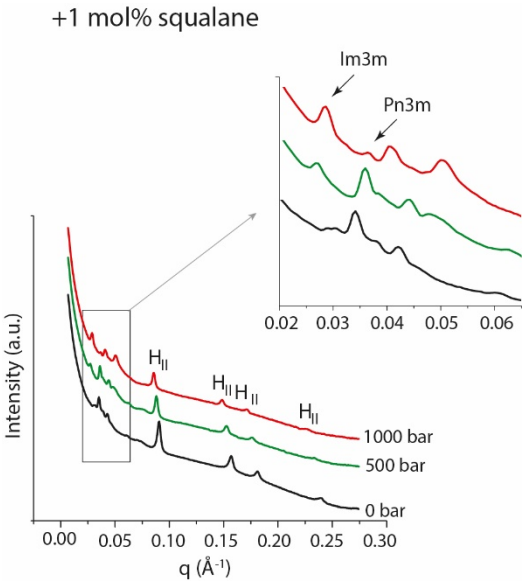

Figure 3. SAXS spectra of the mixture DoPhPC:DoPhPE +1 mol% squalane. At 85°C and ambient pressure (black), 500 bar (green) and 1000 bar (red). Top inset, zoom into the cubic phase region.

325

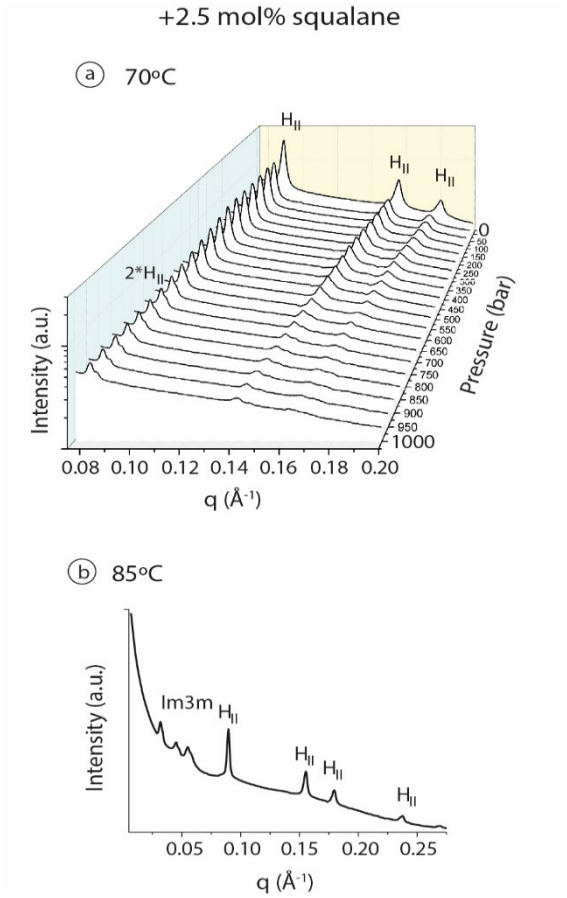

Figure 4. SAXS spectra of the mixture DoPhPC:DoPhPE + 2.5 mol% squalane. a) At 70°C as a function of applied pressure (from 0 to 1000 bar, 50 bar steps). Two H_{II} coexist above 600 bar. **b)** At 85°C at ambient pressure, Q_{II} Im3m and the H_{II} phases coexist.

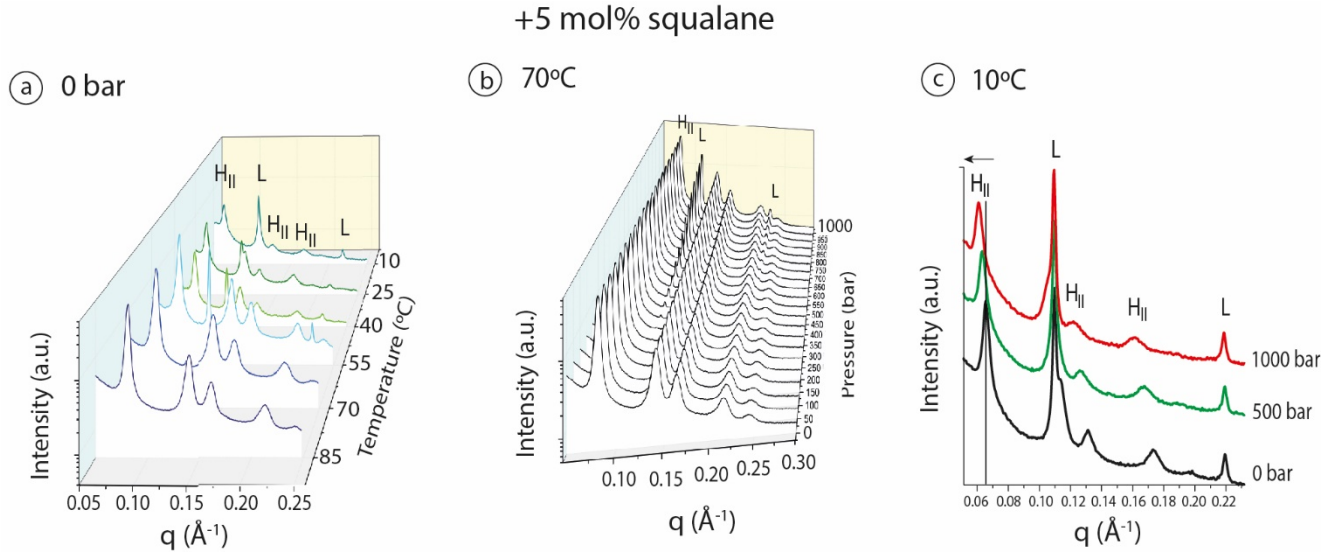

Figure 5. SAXS spectra of the mixture DoPhPC:DoPhPE + 5 mol% squalane. **a)** As a function of temperature at ambient pressure (0 bar applied). **b)** at 70°C as a function of pressure, from 0 to 1000 bar of pressure applied, 50 bar steps. A lamellar phase appears at 350 bar. **c)** At 10°C as a function of pressure. The L and H_{II} phases coexist at ambient pressure (black), 500 bar (green) and 1000 bar (red).

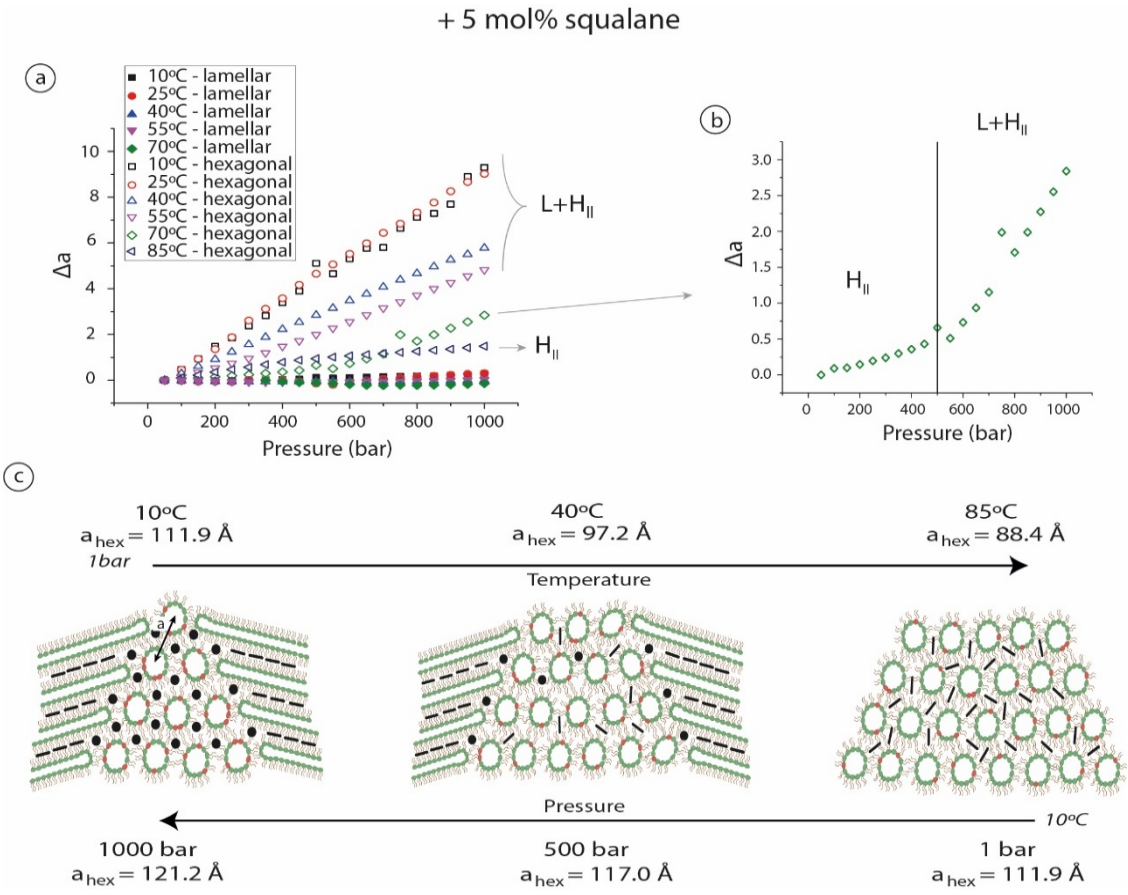

Figure 6. Squalane distribution between lamellar and hexagonal phases. **a)** Normalized lattice parameter (Δa) as a function of hydrostatic pressure. The lattice parameter has been normalized to that at ambient pressure for each temperature. L phase (full symbols); H_{II} (empty symbols). Up to 55°C, both, L and H_{II} coexist. **b)** Detail on Δa as a function of pressure at 70°C. **c)** Schemes of phase coexistence and lattice parameter evolution as a function of pressure and temperature in the DoPhPC:DoPhPE:5 mol% squalane system. Squalane is represented in black, black spheres represent squalane aggregates, lipid hydrocarbon chains are in brown, lipid headgroups are shown in green (PC) and in red (PE).

326

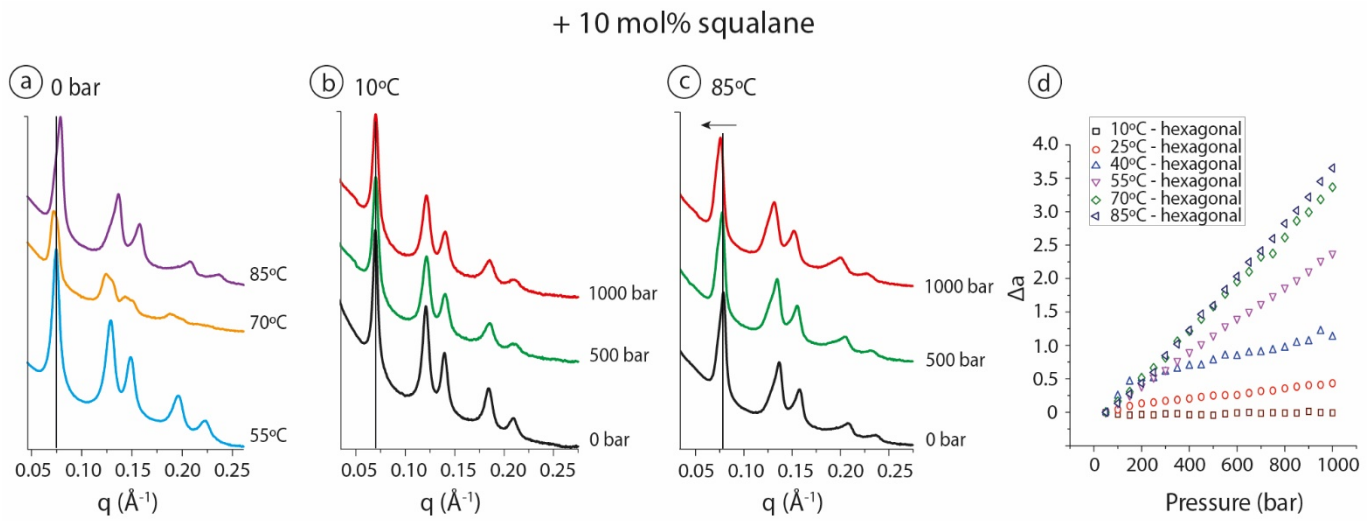

Figure 7. SAXS spectra of the mixture DoPhPC:DoPhPE + 10 mol% squalane. **a)** SAXS spectra at ambient pressure for 55°C (blue), 70°C (yellow) and 85°C (magenta). **b-c)** SAXS spectra at 10°C (b) and 85°C (c) of H_{II} phase as a function of pressure. **d)** Normalized lattice parameter of the H_{II} phase as a function of pressure and temperature. Lattice parameter has been normalized to ambient pressure conditions.

327

Electronic Supplementary Information

Induction of non-lamellar phases in archaeal lipids at high temperature and high hydrostatic pressure by apolar polyisoprenoids

Marta Salvador Castell[a], Nick Brooks[b], Judith Peters[c,d] & Philippe Oger[a]

[a] Université de Lyon, INSA de Lyon, CNRS, UMR 5240, 69211 Villeurbanne, France

[b] Imperial College London, South Kensington Campus, London SW7 2AZ, England

[c] Université Grenoble Alpes, LiPhy, CNRS, 38000 Grenoble, France

[d] Institut Laue Langevin, 38000 Grenoble, France

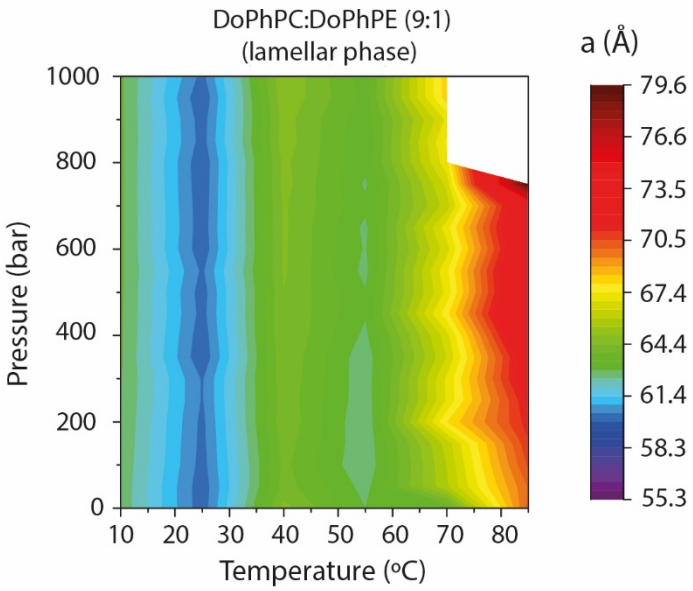

Figure S1. P,T color map of lattice parameters for the lamellar phase of DoPhPC:DoPhPE (9:1).

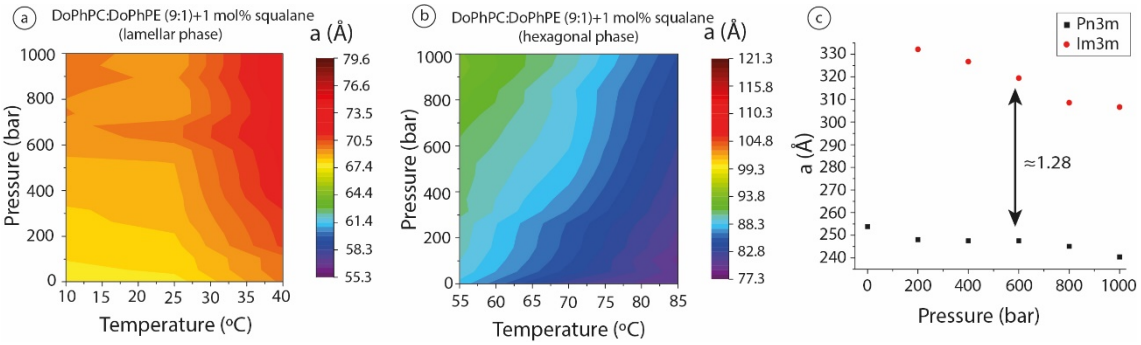

Figure S2. a) P,T color map of lattice parameters for the lamellar phase of DoPhPC:DoPhPE (9:1) + 1 mol% squalane. **b)** P,T color map of lattice parameters for the inverted hexagonal phase of DoPhPC:DoPhPE (9:1) +1mol%. **c)** lattice parameters obtained for the cubic phases Pn3m (black) and Im3m (red) found at 85°C for the DoPhPC:DoPhPE (9:1) +1mol% mixture.

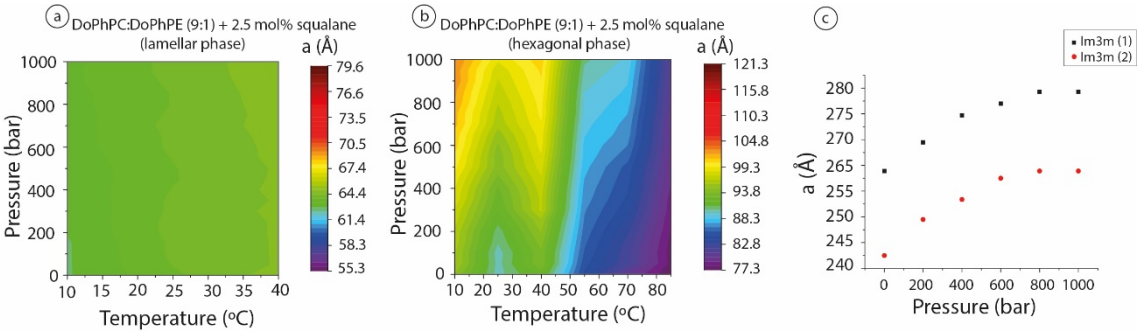

Figure S3. **a)** P,T color map of lattice parameters for the lamellar phase of DoPhPC:DoPhPE (9:1) + 2.5 mol% squalane. **b)** P,T color map of lattice parameters for the inverted hexagonal phase of DoPhPC:DoPhPE (9:1) +2.5 mol%. **c)** lattice parameters obtained for the cubic phases Im3m (red) found at 85°C for the DoPhPC:DoPhPE (9:1) +2.5 mol% mixture.

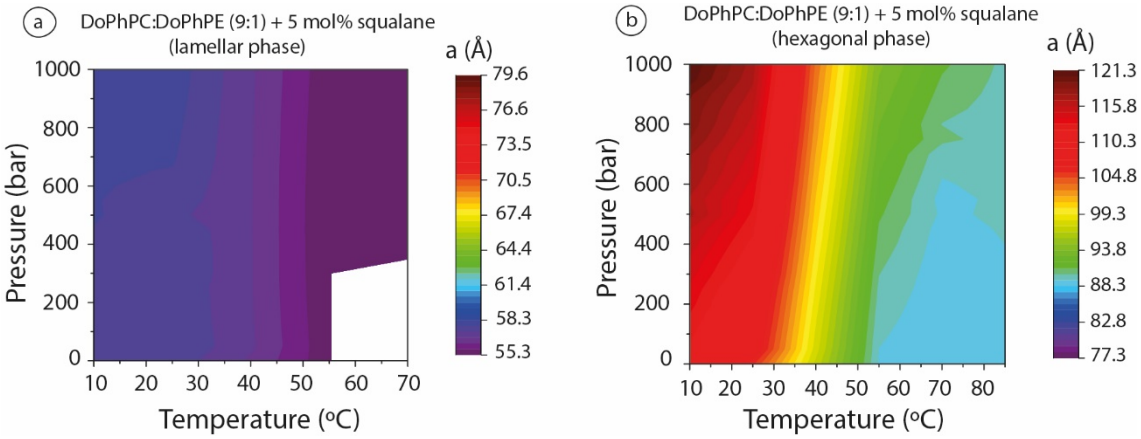

Figure S4. **a)** P,T color map of lattice parameters for the lamellar phase of DoPhPC:DoPhPE (9:1) + 5 mol% squalane. **b)** P,T color map of lattice parameters for the inverted hexagonal phase of DoPhPC:DoPhPE (9:1) +5 mol%.

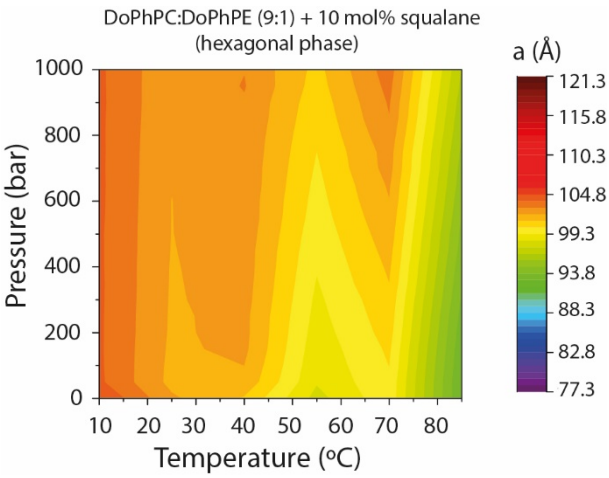

Figure S5. P,T color map of lattice parameters for the inverted hexagonal phase of DoPhPC:DoPhPE (9:1) +10 mol%.